

The “Bering” Small Vehicle Asteroid Mission Concept.

Rene Michelsen¹, Anja Andersen², Henning Haack³, John L. Jørgensen⁴, Maurizio Betto⁴,
Peter S. Jørgensen⁴,

¹Astronomical Observatory, University of Copenhagen, Juliane Maries Vej 30, 2100 Copenhagen Denmark,
Phone: +45 3532 5929, Fax: +45 3532 5989, e-mail: rene@astro.ku.dk

²Nordita, Blegdamsvej 17, 2100 Copenhagen, Denmark,
Phone: +45 3532 5501, Fax: +45 3538 9157, e-mail: anja@nordita.dk.

³Geological Museum, University of Copenhagen, Øster Voldgade 5-7, 1350 Copenhagen K, Denmark
Phone: +45 3532 2367, Fax: +45 3532 2325, e-mail: hh@savik.geomus.ku.dk

⁴Ørsted*DTU, MIS, Building 327, Technical University of Denmark, 2800 Lyngby, Denmark,
Phone +45 4525 3438, Fax: +45 4588 7133, e-mail: jlj@oersted.dtu.dk, mbe@..., psj@...

Abstract

The study of the Asteroids is traditionally performed by means of large Earth based telescopes, by which orbital elements and spectral properties are acquired. Space borne research, has so far been limited to a few occasional flybys and a couple of dedicated flights to a single selected target.

While the telescope based research offers precise orbital information, it is limited to the brighter, larger objects, and taxonomy as well as morphology resolution is limited. Conversely, dedicated missions offers detailed surface mapping in radar, visual and prompt gamma, but only for a few selected targets. The dilemma obviously being the resolution vs. distance and the statistics vs. delta-V requirements.

Using advanced instrumentation and onboard autonomy, we have developed a space mission concept whose goal is to map the flux, size and taxonomy distributions of the Asteroids. The main focus is on main belt objects, but the mission profile will enable mapping of objects inside the Earth orbit as well.

1. Introduction

The keen interest in Asteroids stem from the fact, that these object carry information on solar system and planetary genesis, solar system evolution and history. Most meteorites are samples of main belt asteroids and thus offer a unique chance to study extraterrestrial materials in great detail. Unfortunately, the link between the meteorites and their parent asteroids is poorly understood. This is in part due to the fact that asteroid surfaces are exposed to space weathering which alters their reflectance spectra relative to the meteorites that come from them and in part due to the fact that the asteroid fragments that transfer meteoritic material to Earth crossing orbits are too small to be detected using Earth-based telescopes. What we need, to make full use of the information based on meteorites, is a study of the abundant small asteroids that fill in the gap between meteoroids and km-sized asteroids.

For such a study we have designed the mission named “Bering” after the famous navigator and explorer. It consists of two identical space probes that will fly in a loose formation. Each probe will carry a suite of advanced yet robust instruments that will allow for fully autonomous detection, tracking, mapping and ephemerid estimation of Asteroids. The autonomous instrumentation suite also enable automatic linkup with Earth and inter spacecraft communication. The autonomous operations of the instruments are centered on the Advanced Stellar Compass (ASC). The ASC is a miniature star tracker, that was developed to generate accurate attitude information, but it may also deliver spacecraft velocity and position information. Furthermore, since the ASC autonomously detect any luminous object in its field of view, any Asteroid there will be detected and tracked. Each space probe will carry eight ASC’s to give full sky coverage. The main instrument of the probe is a precision tracking telescope fitted with a multi-spectral imager. When one of the ASC’s has detected an object of interest, the tracking telescope is pointed to the target field via guidance from a dedicated ASC mounted on the secondary mirror of the telescope.

The proposed mission profile encompass a swing-by at Venus. To allow for a comprehensive mapping of Near Earth Objects (NEO’s), the swing-by will take place on the second perihel passage, after which the probes will leave for the main asteroid belt. A subsequent kick burn at aphelion will ensure a proper scanning of the Asteroid belts and ensure a mapping of all Asteroid classes.

The loose formation flying has two objectives. Firstly, it allow for generation of distance information to the target, which otherwise would be constrained only. Secondly, the miniature probe concept will conflict with the need for

redundancy of the main telescope. Because of the autonomous inter spacecraft link, made possible by the ASC’s, only the possibility of stereo imaging of a target is lost should one of the telescopes fail.

This paper describes the scientific scope and expected level of goal achievement, rationale for mission profile, mission stages and the operation of the key technologies. The autonomous operations and estimated performance level of the probes are discussed, based on measured accuracies of the ASC instrument already in-flight, the ASCfit telescope guider and the ASCANT link-up algorithm.

2. Mission objective: A survey of small asteroids – the missing link between meteorites and asteroids

Asteroids and meteorites offer a unique opportunity to study the origin of our Solar System and details of planetary evolution. Photometry of asteroids show that they range from very primitive and ancient bodies in the outer reaches of the asteroid belt to highly evolved differentiated bodies in the inner asteroid belt (Sykes M.V. *et al.*, 2000, Bell *et al.*, 1989). Several of these bodies, including their deep interiors, have been sampled in the form of meteorites.

We propose a space mission to detect and characterize sub-kilometer objects between Jupiter and Venus. The abundance and distribution of these objects is virtually unknown despite their great potential to provide insight to the dynamics of asteroids and in particular the transfer of objects from the main belt to the inner Solar System and the Earth. These small asteroids fill in the gap between the meteorites that we have studied in very great detail in the lab and their large parent asteroids in the main belt that may be studied with Earth-based telescopes. The meteorites have been knocked off their parent asteroids through impacts. These impacts delivered fragments in a large range of sizes – some of them large enough to be detected from a nearby spacecraft like Bering. A survey of these small objects will help us relate groups of meteorites to specific parent asteroids. Studies of meteorites provide detailed information about the chronological, geochemical, and geological evolution of the early Solar System. But unlike geological samples from the Earth meteorites are delivered without any information about the setting of the sampling site. The aim of this project is to link meteorites and asteroids thus providing parent body context to the meteorites and formation details about the asteroids from which they came. The combined evidence will be of great benefit to our understanding of meteorites, asteroids and the origin of our Solar System.

2.1. Meteorites

Meteorites are fragments of approximately 150 different main belt asteroids ranging from highly evolved asteroids with metallic cores, mantles and volcanic crusts to very primitive chondritic type asteroids consisting of loosely agglomerated dust and particles that formed in the earliest phases of the Solar System (Fig. 1, 2). Detailed studies of meteorites allow us to determine age constraints for the formation and disruption of their parent asteroid and the subsequent transfer of fragments to the inner Solar System. Our only means of establishing a link between specific groups of meteorites and their parent asteroids is through a comparison of the spectrum of reflected light from the surfaces of the asteroids and meteorites. These spectra are measures of the mineral composition of the surface of the object and may therefore be used to discriminate between different types of geology. Fig. 3 shows spectra of several different types of asteroids.

Only in one case has it been possible to establish a reasonably good case for a specific asteroid-meteorite relationship. The unique spectrum of the basaltic surface of 4 Vesta makes it the prime candidate for about 400 igneous meteorites known as the HED meteorites. There is considerably interest in establishing links between other groups of meteorites and their parent asteroids.



Figure 1: A fragment of the carbonaceous chondrite Allende that fell in Mexico in 1969. The meteorite is composed of dark finegrained dust, mm-sized spheres and white inclusion known as CAIs. These components formed as individual particles in the nebula prior to planet formation. With an age of 4567 My CAIs are the oldest known solids from the solar system.

Meteorites also provide evidence of catastrophic events in the asteroid belt that may have dramatic consequences for the impact flux on Earth. Today, 38% of all meteorites falling on Earth are L-chondrites. This is probably the result of a catastrophic disruption of their parent body 500 My ago (Haack *et al.*, 1996). Abundant fossil chondritic meteorites in Ordovician limestones from Sweden suggest that the meteorite flux following the event was one order of magnitude higher than the present day flux (Schmitz *et al.*, 1997).



Figure 2: A 30 cm wide slice of the pallasite Imilac. Pallasites are stony iron meteorites that probably come from the boundary between the metallic core and stony mantle in differentiated asteroids. Unlike the asteroid from which Allende came from the parent asteroid of Imilac was heated to the melting point of the metal phase thus causing differentiation of the body into core, mantle and crust. Note the completely different origin, evolution and appearance of these two types of meteorites. A-type asteroids could be composed of pallasite like material. Geological Museum, University of Copenhagen.

Another example is the IIIAB iron meteorites that are the most common type of iron meteorites falling on Earth. IIIAB irons probably come from the catastrophic disruption of a large differentiated asteroid 650 My ago (Keil *et al.*, 1994).

Observations of larger fragments from these events will constrain the orbit of the original asteroid and the rate at which the fragments are being dispersed in the Solar System.

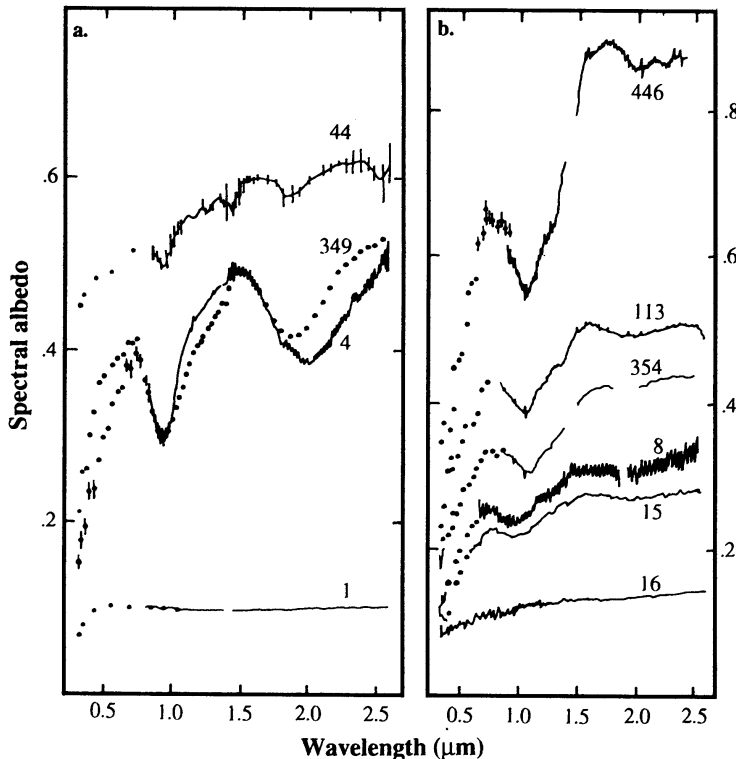


Figure 3: Selection of asteroid reflectance spectra illustrating the diversity of asteroid surface properties. Spectra are shown for 1 Ceres a C-type asteroid that could be the parent body of carbonaceous chondrites like Allende (Fig. 1); 4 Vesta a V-type that is probably the parent body of the basaltic HED meteorites; 8 Flora, 15 Eunomia, 113 Amalthea, and 354 Elenora are S-types that could be parent bodies of ordinary chondrites; 16 Psyche is an M-type that could be the exposed metallic core of a differentiated asteroid; 349 Dembovska is a rare R-type asteroid with no known meteorite analogue; 446 Aeternitas is one of the rare A-type asteroids which are rich in olivine and probably represent fragments of mantle or core-mantle boundary material. From Michael J Gaffey, Jeffrey F. Bell, and Dale P. Cruickshank (1989) Reflectance spectroscopy and asteroid surface mineralogy. In Asteroids II, University of Arizona Press, 98-127.

2.2. Transfer of material from the asteroid belt to the inner solar system

NEO's are objects with $q < 1.3$ AU that may make encounters with the Earth or even impact the Earth. NEO's therefore also include all meteoroids that will fall on the surface of the Earth in the form of meteorites. The population of NEO's is a transient population of objects that is believed to be in a steady state situation where the supply of new members balances the number lost. Due to the perturbations from the planets in the inner solar system NEO's have typical lifetimes of 10^7 - 10^8 y. Some of the NEO's collide with the terrestrial planets but most of them either collide with the Sun or become ejected from the Solar system after a close encounter with one or more of the planets (Bottke *et al.*, 2002). Most of the NEO's are believed to be asteroids that originated from the main asteroid belt (Morbidelli *et al.*, 2000). A minor fraction of the NEO's are derived from comets.

The two main transfer mechanisms from the asteroid belt to NEA's (Near Earth Asteroids) are the ν_6 secular resonance and the 3:1 mean motion resonance (Fig. 4) (Froeschlé and Morbidelli, 1994; Moons, 1997). Asteroids in these resonances undergo a fast (time scale $\sim 10^6$ y) orbital evolution due to interactions with one or more of the planets until a planetary encounter or collision removes them from the resonance.

Since the resonances are continuously drained for material, other processes are required to supply fresh material into the resonances. The asteroid belt is continuously undergoing a collisional evolution that occasionally involves larger collisions between asteroids. Fragments from these collisions may end up in orbits that are resonant with Jupiter and/or other planets. Smaller asteroids may drift toward the resonances due to the Yarkovsky effect (Farinella *et al.*, 1998). Finally, meter-size objects spiral toward the Sun due to Poynting-Robertson drag.

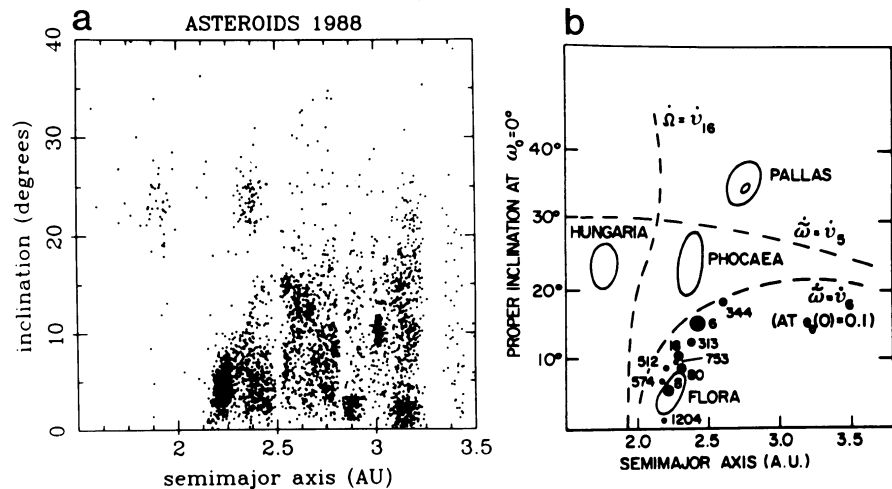


Figure 4: *a)* Distribution of asteroids in the main belt. Note the sparsely populated mean motion resonances at 2.5 AU (3:1), 2.82 AU (5:2), 2.96 AU (7:3) and 3.28 AU (2:1). *b)* Location of secular resonances in orbital space. Note the $\dot{\nu}_6$ resonance which defines the upper limit of the densely populated areas of the main belt in *a)*. From Froeschle and Greenberg (1989).

2.3. Sub-kilometre asteroids

We have very little information on the abundance and characteristics of objects smaller than about 1 km except for those that have been observed in the immediate vicinity of the Earth. The power law distribution of asteroid sizes (Fig. 5) suggests that objects smaller than 1 km should be very abundant. Furthermore, the orbits of these small objects are easily perturbed and we should therefore expect to see them more or less uniformly distributed throughout the Solar System. Within the asteroid belt we have no information at all since such objects cannot be observed from Earth and no spacecraft has been actively looking for them.

Small objects provide important information on the dynamics of asteroid material for three main reasons:

1. The orbits of small objects are quickly perturbed due to the Yarkovsky effect and Poynting-Robertson drag leading to shorter lifetimes than regular asteroids. The abundances of small objects close to and within the resonances are therefore measures of the current production rate of smaller fragments.
2. In contrast to the larger asteroids studied from space so far, small objects are unlikely to be regolith covered, their surface spectra may therefore more easily be related to that of the corresponding meteorite type.
3. Some of the small objects come from the same asteroidal source as the meteorites that have already fallen on Earth. Data on the orbital distribution of objects with spectral characteristics similar to a group of meteorites will provide new constraints on the meteorite/asteroid relationship. The so-called Vestoids is an

example of a group of small objects for which a combination of their spectral characteristics and orbit parameters have been used to establish a link between the members and their parent asteroid, Vesta (Binzel *et al.*, 1993). Vestoids are 5-10 km V-type asteroids that form a stream in orbit space from Vesta toward the 3:1 mean motion resonance. Vestoids are believed to represent large fragments that were ejected from Vesta in a major impact event. Those fragments that made it to the 3:1 resonance are believed to be the parent bodies of HED meteorites. We infer that sub-kilometer objects that are considerably more abundant than 5-10 km objects will be even better to establish links between fragments and their parent asteroid. For the Vestoids, detection of sub-kilometer V-type fragments will help constrain the efficiency of the Yarkovsky effect that operates faster on smaller objects.

Constraints on the abundance of small objects will also allow much better age determinations of planetary surfaces such as the very young lava flows (< 10 My) on the northern plain on Mars. In the absence of documented samples from the planetary surfaces the only means of determining the age is by impact crater counting. The big problem is that an age estimate also requires knowledge of the impact flux. This again is closely related to the abundances of different sizes of asteroids which is one of our main objectives. Better ages for such surfaces will provide new insight on the geological evolution of the terrestrial planets and Moons of the outer Solar System.

2.4. Kilometer-sized asteroids

Kilometer-sized asteroids are large enough to present a significant hazard, yet small enough to escape most ground-based surveys. Although they are not the primary target of the proposed mission we estimate that we will detect 5-10 of such objects per year. Depending on the position of the objects relative to the Earth at the time of discovery it should, in some cases, be possible to track the objects with ground based telescopes.

In the few cases where the object is sufficiently large and close to Bering, the science telescope will be used to record a series of ultra-spectral images of the object as it rotates within view. These images will be used to study the age and the geological evolution of the object. A very interesting possibility is to plan a flyby of an M-type asteroid (metallic asteroid). This would be the first flyby of such an object and provide us with the first pictures of the surface of an object unlike anything we have ever seen before. We have basically no idea what an impact crater on a solid metal object would look like but we have every reason to believe that it would give us something to think about. Another aspect of these asteroids is that they would be prime targets for mining operations in the distant future.

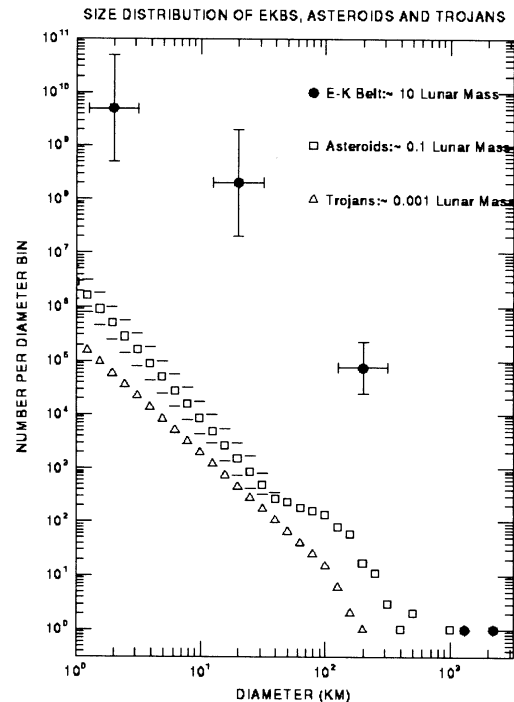


Figure 5: Inferred size distribution of asteroids (open squares) based on ground based surveys (From Davis *et al.*, 1997).

2.5. Detection rates

The detection rate of the Bering spacecraft, i.e. the number of visible objects (for which astrometry as a minimum is possible) per day, depend critically on both the size-distribution of the asteroids, as well as the detailed mission profile. A rough estimate of the detection rates serves as initial input for the functional requirements of the spacecraft. However, as the size distribution of the sub-kilometer asteroids is completely unknown, the detection rates must be carefully evaluated against several different size-profiles, ranging from a conservative to an over-optimistic profile regarding the total number of asteroids, expecting the truth to be somewhere in between. By a numerical integration of the orbits of the spacecraft and different populations of test particles during a given phase of the mission profile, we hope thus to be able to fix some very firm limits for the detection rates. This work is currently in progress.

3. Functional requirements

The objects to be studied are unknown, so the probe must detect the objects and guide the science instruments in a fully automated process. It is estimated that a reasonable detection rate (i.e. several detections/day) requires that the detection limit of Bering should be better than $m_v = 9$.

In order to determine the distribution and dynamics of small objects, we need to detect objects in the main asteroid belt as well as inside the Earth’s orbit, we therefore propose an orbit that would give us data on the distribution of small objects all the way from 0.7 AU to 3.5 AU.

For each detected object we propose to autonomously determine:

1. The heliocentric position, and velocity vector of the object;
2. Photometry of the reflected light from the object in the 350 – 2200 nm range;
3. The light curve of the object and thereby its rotation period.

For a few selected larger objects we, furthermore, propose to:

1. Record multi-band images of the surface;
2. Determine the mass and magnetic moment of the object.

The data will allow us to determine a current orbit for the object. With a detection limit of $m_v = 9$ for the Advanced Stellar Compass and a detection limit of $m_v = 25$ for the multi spectral imager we will be able to follow the object out to a distance of approximately 2×10^6 times the distance where it was detected. Depending on the geometry this will typically allow us to follow the object for weeks to months and determine high precision orbital parameters for a large fraction of the orbital arc. The orbital data will also allow us to determine the objects position in orbital space and its proximity to resonances and/or other asteroids or asteroid families with similar spectral characteristics.

The photometry will allow us to determine the spectral type of the object. This will make it possible for us to determine its relationship with other asteroids and/or groups of meteorites (Bell *et al.*, 1989) with similar mineralogy. Ultimately, we will attempt to backtrack the object to its parent asteroid.

The ability to detect objects down to $m_v = 25$ from within the asteroid belt with the multicolor imager may also be utilized to further constrain the density of small objects. In a few campaigns we plan to take series of frames with either subsequent data processing either onboard or on ground. This will allow us to determine the number of asteroidal objects in each frame, down to very faint objects. Although the size-distance relationship cannot be determined on the basis of a few frames these data may be used to check predictions based on models of the distribution of asteroids.

A number (10+) of probe magnetometers will be launched toward selected and suitable target asteroids. The magnetometers will provide information about the distribution of the magnetic field, and as such probe the interior of the asteroid.

4. Instrumentation

At a distance of 3AU the closed loop to Earth is approx. 48 minutes. Furthermore, the link budget at this distance is rather limited. It is therefore obvious that the instrumentation payload for the Bering spacecraft will have to possess a high degree of autonomy. Also, the autonomy must encompass all everyday routines, such as object detection, classification, tracking and initial data acquisition. Only in the rare cases, where a large or otherwise scientifically interesting body happens to come close to the spacecraft, ground intervention may be considered. The science requirements set forth above, will thus involve three steps.

1) Detection: The autonomous object detection shall be able to pick up all approaching objects of interest at a suitable distance that permits an efficient observation scheme of the object during the time of passage of the object. This objective generates two design drivers. Firstly, the instrument that makes the initial discovery of a new object must be able to work for distant, i.e. faint objects. Secondly, the instrument must cover a large fraction of the sky in order to minimize the number of objects slipping by the spacecraft unnoticed or detected too late.

2) Tracking: When an object is positively detected, the object has to be tracked so as to obtain its orbital parameters and at the Closest Point of Approach (CPA) to perform the science classification. To perform this efficiently and fully autonomously, three steps are involved. At an early stage, the object shall be pre-classified so as to assign a figure of merit for its further tracking history and importance. This classification requires an approximate assessment of the object size, type and time to CPA. Secondly, observations of the object position and velocity for a

precise assessment of the orbital parameters must be estimated. Finally, in case of judging the object to be of high interest, a message should be dispatched to Earth.

3) Science observation: About the time of the CPA in the standard case, or in case of a poor illumination phase calculated at CPA, while sufficient illumination phase still exists, measurements of the physical parameters derived from the scientific objectives, shall be measured. The observables to be collected are: high-resolution multi spectral images, albedo assessment, size, rotation state, and if possible magnetic signature.

Based on this breakdown of the scientific requirements, we arrive at an instrumentation package as given below. It is worth noting, that while the package has been optimized for a slowly rotating spacecraft, it may, with modifications be adapted to a fully three axis stabilized spacecraft. The reason for optimizing for the slowly rotating mode of operations is that this approach minimizes the number of moving mechanisms, instruments and control devices.

4.1. Advanced Stellar Compass

The Advanced Stellar Compass (ASC) is a fully autonomous lightweight, miniature, low power robust star tracker with extensive flight heritage (e.g. ØRSTED, CHAMP, PROBA, GRACE, ADEOS-2). The system typically consists of two CCD miniature Camera Head Units (CHU) backed by a powerful processing unit. Its basic operation is to deliver timely and accurate attitude information. This information is used, both closed loop by the attitude control system, and as an inertial attitude reference for the science instrumentation.

The ASC operates by matching observed luminous objects in the Field of View (FOV) to a star catalog database. In the standard configuration, the star catalogue contains the 14,000 brightest stars (i.e. complete to $m_v = 7.0$) but catalogues to 200,000 have been tested. If a catalogue of, say, 165,000 stars is used, it is complete to $m_v = 9.3$.

The performance envelope of the instrument is roughly 1" in pointing and 7" in rotation at a 2Hz update rate. However, by combining the attitude from more than one camera unit, the overall attitude accuracy will be as low as 0.7" at 2Hz and at end-of-life. Furthermore, in case that several instruments require very high accuracy attitude data, additional camera heads may be added to the design at a marginal mass penalty.

Because the ASC analyses all luminous objects in the FOV and matches these to the catalogue, it will also detect which objects are NOT stars, i.e. non-stellar-objects (NSO). At $m_v = 9$, the list of NOS from each image includes several galaxies, nebulae, etc., as well. The accuracy of an $m_v = 9$ object is about 7" (extended sources are slightly worse).

During the qualification of this process, we have tested two different schemes to remove the deep space objects from the list, which show similar performance. The one is to compare observations from a time series of observations of the object, and then to remove anything that does not move a certain distance per time. The other is to update the star catalogue with any object that does not move on a timescale of days. Both methods efficiently remove any slow moving object.

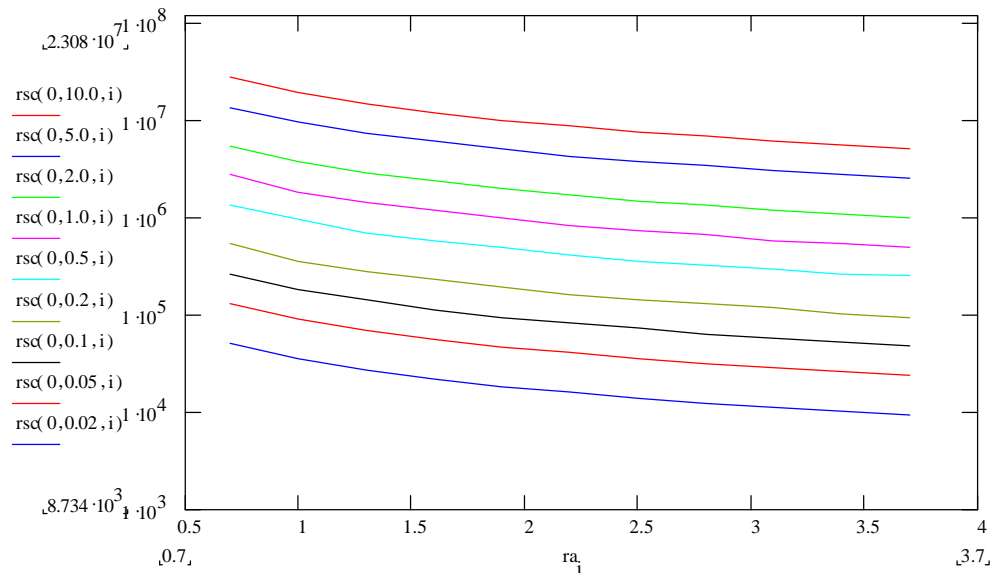


Figure 6: Shows the maximum detection range for meteoroids of various sizes vs. distance to the Sun. At 0.7AU, a 10km meteoroid will be detected as far as 22 million km away, whereas the same meteoroid will only be detected when closer than 6 million km at 3.7AU. A 20m meteoroid will have a modest 10,000km detection range at 3.7AU.

During a satellite rotation, each ASC camera head will make multiple observations of any non-stellar object brighter than $m_v = 9$. Assuming a rotation speed of 1 rev. per hour and an update rate of 1Hz, each object will then be observed more than 100 times, thus enabling both an increased position accuracy and an angular rate estimate. The ASC may simultaneously handle 500 such objects per image. The plan is to have each ASC camera sending the non-stellar object list, filtered for deep space objects, to the central computer for further onboard processing.

Using the proven ASC detection capacity and reasonable assumptions for the surface reflection properties of the asteroids, the detection range may be estimated. Fig. 6 shows the maximum detection range for meteoroids of various sizes vs. distance to the Sun.

The next generation micro Advanced Stellar Compass (μ ASC), is currently being developed. Apart from improved processing power, lower mass and power consumption the μ ASC will allow for integration of additional data processing such as other science sensors. These features will make the μ ASC ideal for the Bering mission.

4.2. Multi spectral imager

The main science instrument on Bering will be the telescope aided multi spectral imager. In front of the telescope a folding mirror provides the possibility to actively point the imager FOV.

4.2.1. Telescope

The dimensioning of the telescope for the multi spectral imager basically has to be determined by balancing two independent but conflicting requirements: Firstly, the capability to fully autonomously acquire and track an object, as soon as it has been detected by the ASC’s. Secondly, the capability to obtain high-resolution multi spectral images of the scientific interesting targets at large distances. The first suggests a telescope with a moderate focal length where-as the second drives for a large focal length.

Aperture: Both of the above requirements drive for a large entrance pupil. However, the mechanical structure and ruggedness of the folding mirror will set the maximum size of the entrance pupil. The folding mirror size scales roughly with the product of the entrance pupil and the size of the tracking angle span.

A telescope with an entrance pupil of diameter 25cm, will have a tracking capability that allows the telescope to track an object far more distant than the ASC. So, although the science imaging most likely will take place at, or near, the closest point of approach, the objects will be tracked long after they have left the detection sphere of the Bering mission, as depicted in Fig. 7. Analysis shows that the tracking range to detection range ratio is approximately a factor of 4. This means that the telescope will be able to track a 10 km meteoroid at up to 80 million km distance, corresponding to 10-100 days of tracking.

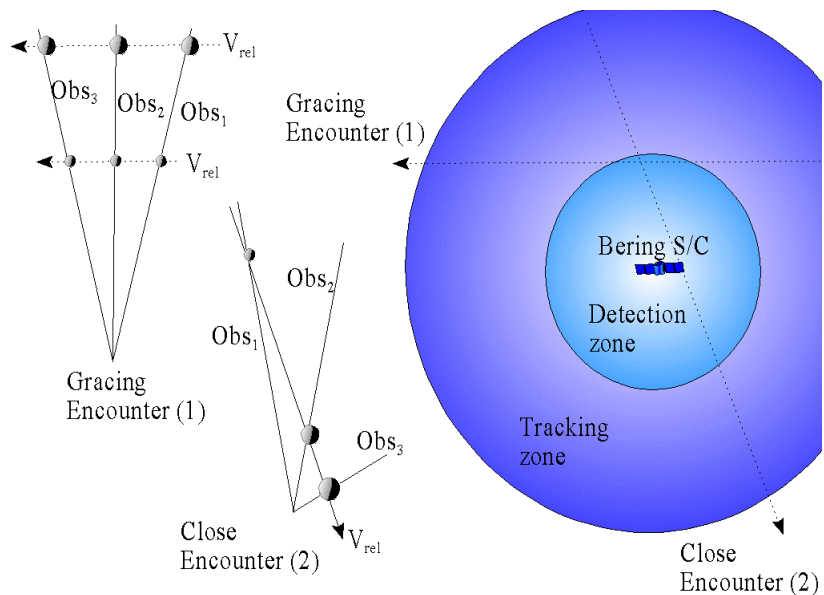


Figure 7: Meteoroid encounter detection and tracking range.

Focal length: The Airy dish for a 0.25m pupil is in the range of 1"-3" for the wavelength in question.

Assuming a pixel size of 6.5 μ m and some 1400 pixels with, the tradeoff between lock and track capability and the science image resolution may be assessed. A 1.0m focal length will result in a FOV of 30 arcminute, and a pixel size, of 1.3". From tests of the ASCfit module, using an ASC and a 2.2m telescope with various focal lengths, it is found that a 30' FOV is easily locked on to. On the other hand, the image of a 10km target will cover 1 pixel at 1.5 million km distance, and will give an image of 100 pixels at 250,000 km. The spacecraft rotation will force the target through the FOV in 5 seconds, which limits the maximum integration time to 1sec, with the tip/tilt mirror at rest. Considering a 2m focal length twice the resolution is obtained, but the maximum integration time will then

drop to 0.5 seconds, thus reducing the tracking depth by a factor of 1.4, and at the same time, the overall length of the telescope, assuming a simple Cassegrain layout, will approach the limit set by the spacecraft size.

Tracking: The meteoroid tracking accuracy using the telescope is roughly improved by the ratio of resolutions of the telescope over the ASC, this means that, at the maximum tracking distance of the telescope, the “per sample” accuracy will be about 50-100" cross track depending on the choice of focal length. Because of the absolute nature of the observable, the noise of these measurements is Poisson limited, thus leading to a noise reduction of $(N)^{1/2}$ from N samples. For larger objects, the number of samples will be several thousands, leading to a cross track accuracy in the range of milliarcseconds.

However, as depicted in Fig. 7, where a grazing close encounter is shown, the radial component of the meteoroid velocity, in the spacecraft rest frame, may not be recoverable. The problem is, that a near and slow object may be mistaken for a fast and far, i.e. the so called *aperture problem* of imaging.

The aperture problem is trivially resolved if the two spacecraft perform simultaneous observations of the object. There are two possible configurations: relatively close and far formation. The proposed laser ranger (see below) can also alleviate this for objects that come closer than 10.000km

The “Close” formation, with spacecraft separated by 10-20% of the detection zone, has the advantage that the object is automatically detected by both spacecraft simultaneously, and the matching is trivially performed. The obtainable accuracy of the position and velocity estimates depends on the range and distance from the symmetry line of the two spacecraft.

The “Far” formation, having a larger baseline features both better accuracy and a larger volume of search. However, since the target will only be within the detection volume of the one spacecraft, the telescope of the other will have to actively search for the target.

The optimum formation distance depends on the size of the target objects that scientifically is defined to be the most important. Because the delta-V required to change the formation is quite marginal (5-20m/s), it may therefore prove to be desirable to design 1-2 month campaigns optimized for certain range of objects.

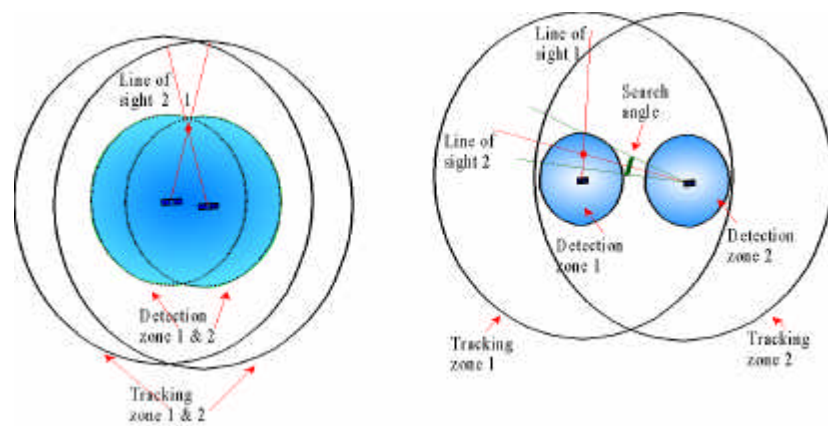


Figure 8: Close and far formation flying.

4.2.2. Imager

The multi-band imaging system of the Bering satellite is designed to acquire unique information of the asteroids. The multi-band images will contain important information of the surface composition. By combining the image information with the laser ranger output the spatial extent for the asteroids can be determined. By monitoring an asteroid through a series of images, information about its rotation state can be obtained. The short term orbital elements can be obtained from a high precision tracking of the asteroid over time which can enable astronomers on ground to point ground based telescopes towards the observed asteroid.

The 6-band, digital imager will cover a broad wavelength band, from infrared (2200 nm) to near-UV (350 nm), in order to optimize the scientific value of the recorded images. As depicted in Fig. 9, the imager consists of a primary telescopic mirror that collects light from a tracking folding mirror and projects it onto a secondary mirror.

Through an opening in the telescope canister, the collimated light from the secondary mirror is sent into two separate three-band imagers; one covering light in 'visible' wavelengths, the other, placed inside a low-temperature (100K) box, covering the infrared band.

In each of the three-band imagers, two dichroic mirrors separate the incoming light into the chosen wavelength bands and project the beam onto the image sensors, where additional filters provide further chromatic separation in

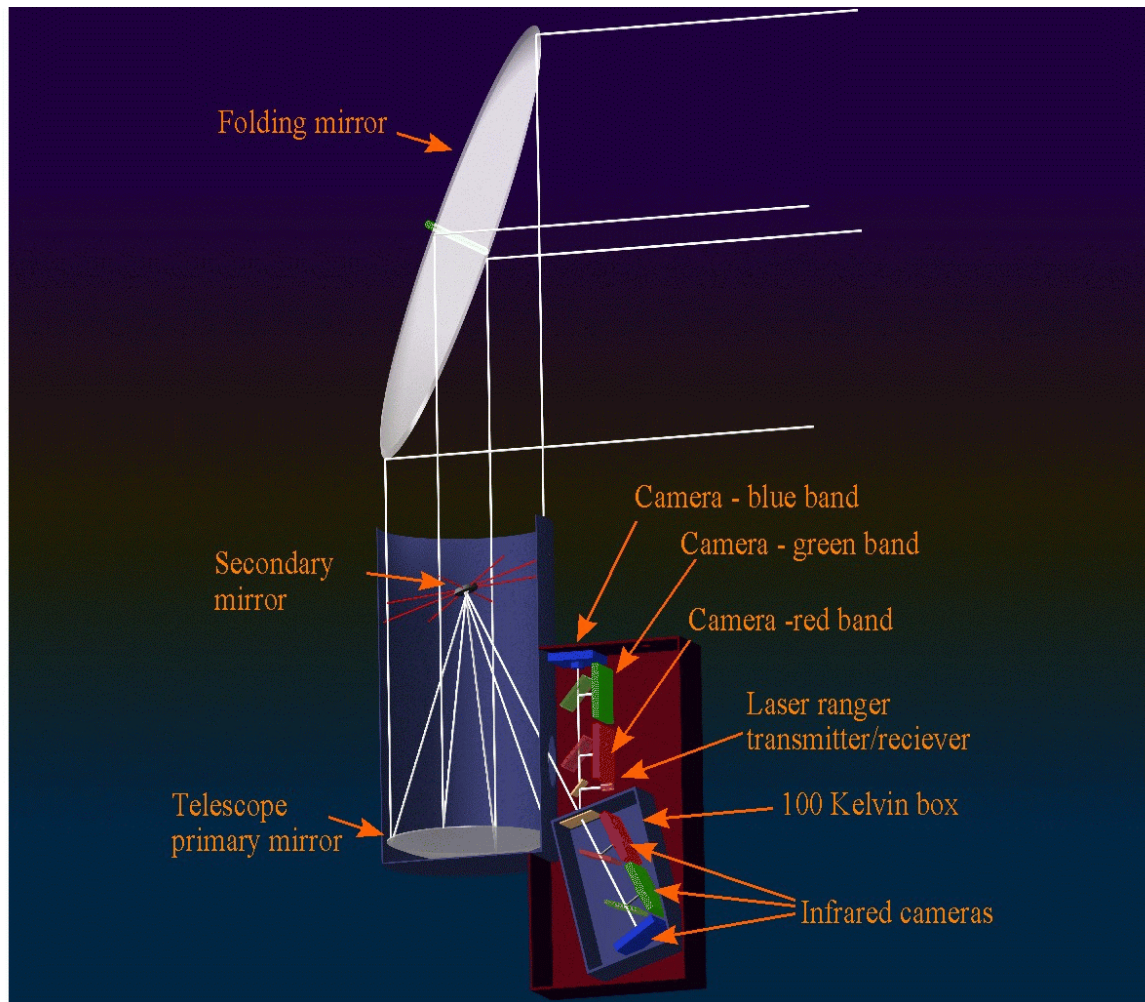


Figure 9: The Bering imager system.

accordance with mission requirements. The wavelength bands will enable a first order spectral classification of the objects in the FOV.

4.3. The Laser ranger

Depending on the choice of main computer, the capability of handling simultaneous tracking and categorization of multiple science objects is limited. A reasonable number will be less than 200 simultaneous targets for a processor similar to the PROBA spacecraft main processor. In order to enable a rapid distinction between large and small objects, a laser-ranger instrument has been included in the instrument package. This instrument will give instant distance information of near targets, whereby the object can be classified, and its future observation program established. A smaller object in the meter class may then be detected, ranged, spectrally classified, and excluded from further science processing. This will free up the main telescope to focus on the more interesting objects in range. The above process can be handled fully autonomously with a very high level of robustness. On the other hand, if no large science objects are in range, the focus can dynamically (or manually during campaigns) be shifted towards smaller objects, so that the observation time is used optimally at any given instant.

The contemplated laser ranger will have a limited measurement range, mainly set by a fairly conservative transmitter/receiver design. The principle of operation is as follows: The laser transmitter uses the telescope and tracking facility of the multi spectral imager as beam-expander and pointing device. Obviously, the laser will have to be synchronized to transmit in between image acquisitions. Assuming that the telescope is locked on a target, the laser will send out a short pulse through the telescope to the target. The pulse will hit a fairly small spot on the target, which then reflects a fraction of the light. The part of the light that returns to the telescope will be focussed on a small fast receiver. By measuring the time of flight for the pulse the distance is found.

The components of the design we propose do all have substantial space heritage. Assuming a LED pumped Nd:YAG Q-switched unit is proposed as laser source, and a simple avalanche photo diode as sensor, a system having 15m resolution for 20nsec pulses is fairly easy realized (JHU/APL, 1998). The range of the sensor is largely set by the limited Signal to Noise (S/N) ratio between the laser pulse photons and the detector noise and solar illumination photons. To minimize the latter, the detector is fitted with a narrow band spectral filter (note that the 5km/sec relative velocity give negligible Doppler shift). Assuming a pulse energy in the range of 0.2J, a S/N well above 50 is achievable at 10,000km range at worst case conditions, i.e. 0.7AU, Sun, S/C and target on line and low target albedo.

The proposed design has substantial advantages over similar designs used on other spacecraft. First, the accurate pointing of the telescope minimizes the pulse widening from slant angles. Secondly, the use of the telescope allows for a very small spot size. Thirdly, thermal effects on a high precision optical system as a laser ranger, is typically limiting both accuracy and range. Especially the return beam will have to be fairly accurately positioned in order to be focussed on the extremely small aperture of the detector diode. Because the actual coordinate to be tracked by the telescope does not have to be the center of the target, and may be changed in flight, the consequence of thermally induced shifts is marginal.

4.4. Gravity probe/Magnetometer probe

A few objects will be big enough and pass close enough such that a small magnetometer probe can be ejected and tracked from Bering as it passes close to the object. The deflection of its orbit will allow us to constrain the mass of the object.

Assuming a relatively large asteroid approaching the mother satellite a Free-Flyer Probe could be ejected with a v of 10m/s towards the asteroid. Using the reflected light of a pointed laser beacon, the Bering telescope will track the probe and record any changes in the trajectory.

Fig. 10 shows the situation for the estimation of the asteroid mass. After a small fine-tuning of Bering trajectory, the probe is ejected. The probe is equipped with cats-eye reflectors so that the reflected laser-light will make the probe visible on the images taken with the science telescope. As both probe and Bering flies on undisturbed, the Bering telescope will see the probe in a constant direction relative to the background of the fixed stars. When the probe is at its closest distance to the asteroid it will experience an impulse-like force, giving rise to a change of the probe velocity, which on the Bering telescope images is seen as a post encounter drift. The gravitational deflection is indeed impulse-like when considering relative velocities between the asteroid and the probe larger than 1km/s for asteroids of 1km radius.

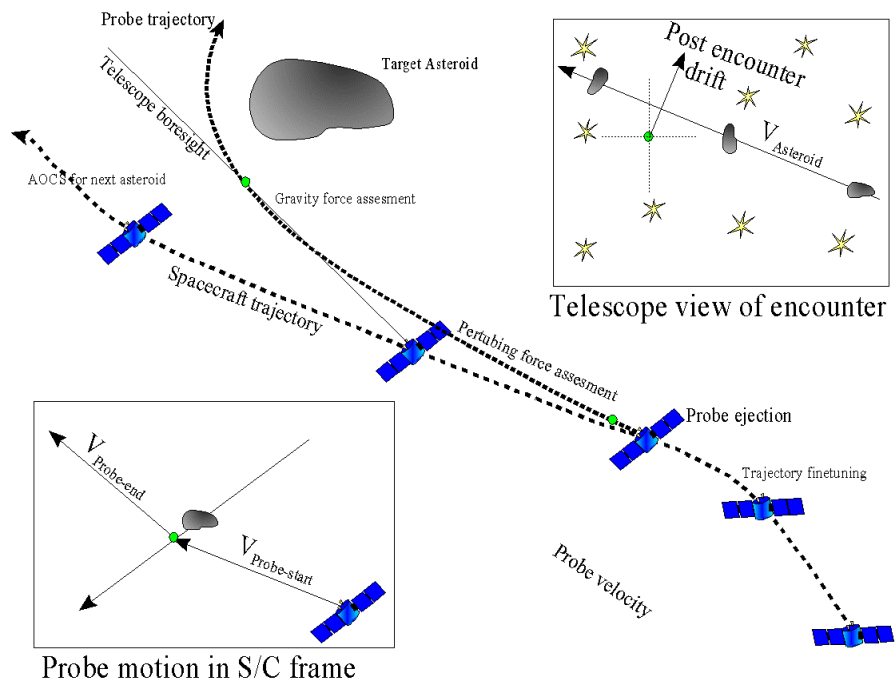


Figure 10: Principle of mass estimation.

The estimated post-encounter angular drift-rate (in mas = milliarcseconds) is shown in Fig. 11. The estimate is made for a 1km asteroid having a mass of $M_A=1.25 \cdot 10^{13}$ kg and a closest distance between asteroid and probe of $d_{min}=100$ km. The contour levels scale with the factor (M_A/d) . The maximum reliable distance measurement of the laser ranger is to be considered 15.000km. At this distance an initial uncertainty of 0.25° in the direction of ejection

will give 65km uncertainty in the position of the probe. The minimum distance between probe and asteroid of 100km is therefore a conservative estimate and might be as lower, when trajectories are favourable.

Angular drift-rates of 1-10mas/day will be observable when performing high accuracy astronomy on the images taken with the science telescope. The principle has been demonstrated on ground with the ASCfit software package fitting astronomical coordinates to images using catalog information. It is expected that the relative accuracy on images with close to identical star patterns will be better than 10mas. Averaging over observations covering several days will further increase the accuracy.

Being able to fix the position of the probe to 10mas at a distance of 20,000km corresponds to a cross-line-of-sight accuracy of 1m for the position of the probe relative to the Bering S/C. In the along line-of-sight a corresponding level of accuracy is expected from the laser ranger. Thus it will be possible to fix the probe position within a 1m³ error-box. Corresponding accuracy can be obtained for the asteroids that are luminous enough to be observed by the science telescope.

The second objective of the probe magnetometers is to search for and characterize the magnetic field of the asteroids encountered.

Kivelson et al. (1993) extrapolated magnetic field measurements obtained at the closest approach of Galileo at 1600 km or 230 Gaspra radii, and estimated the surface field to be between 4000 and 140,000 nT (the surface field of the Earth is between 23,000 and 70,000 nT). The free-flying magnetometers ejected toward selected asteroids will be able to provide the first opportunity to explore a complicated miniature planetary pseudo-magnetosphere, and in this way provide a link to the natural remnant magnetization measured in meteorites (Sugiura & Strangway 1988).

Taking a 10 km diameter asteroid of Ni-Fe alloy (4.39×10^{15} kg) and assuming that the asteroid has been partly magnetized, e.g. by an ancient collision of another celestial body, the magnetometer will measure a magnetic signature at the rendezvous. Say a localized $10 \times 10 \times 0.5$ m-volume of the asteroid has been fully magnetized ($m_m = 63.7 \times 10^6$ Am²) the polar field from the equivalent dipole is ~ 80 μ T at a distance of 100 meter. The probe will measure a signature of 40-80 μ T if the magnetized volume happens to be just above the probe as it is flying by. On the other hand, if the volume is on the other side of the asteroid (10 km) the magnetic signature on the free-flyer magnetometer is only 40-80 pT.

The basic operation of the Bering Free-Flyer probes is fairly straightforward. It is mainly a one way data logger, taking magnetometer measurements and transmitting them via a radio-link to the main satellite. In order to save power the probe will be ejected in stand-by mode and at the asteroid encounter a light sequence from the laser will switch on the probe. In addition to the electronics required for the magnetization diagnostics, the probes require a structure covered with a high reflecting mantle for the gravity diagnostics: Probe dimensions $\varnothing 40 \times 200$ mm³; probe mass 300 g; probe power 400 mW and probe lifetime 3 hours and 30 days standby (using high-capacity LiSOC₁₂ batteries)

In order to carry a multiple number of probes but at the same time being able to track a probe at a distance of +10,000 km the probe is considered having a size of approx. 10^{-3} m³. The structure of the probe will have a cylindrical shape, having the magnetic sensor in one end and the electronics in the other, to reduce magnetic contamination. The structure must be properly balanced to provide a steady platform when the probes are spin

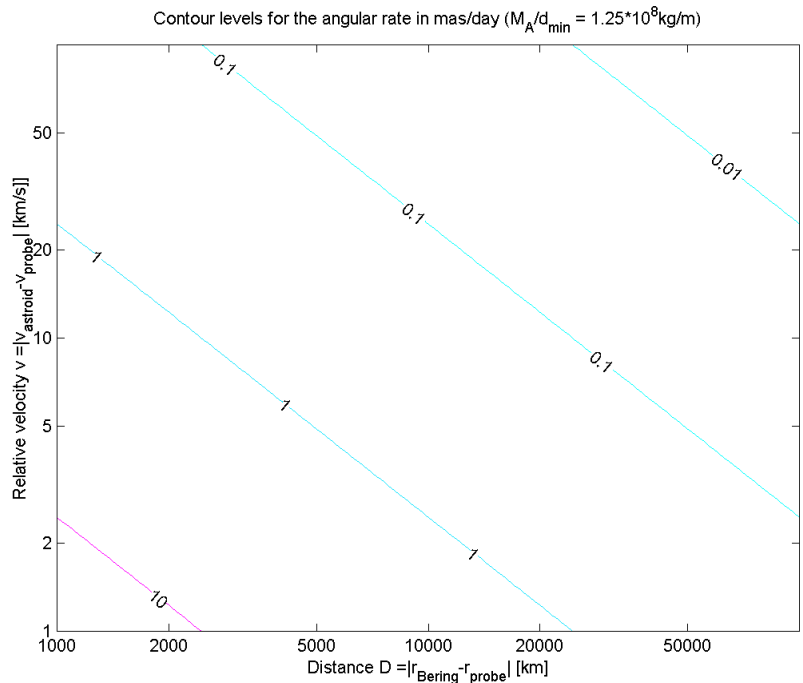


Figure 11: Estimated post-encounter angular drift-rate.

stabilized, and provide damping of the mechanical impact of the electronics when the probe is ejected. The electronics will be mounted in epoxy in order to damp the large impact from the howitzer when ejected.

5. Mission profile

In order to accomplish the mission goals the Bering spacecraft shall search both the inner part of the solar system and the main asteroid belt with a serendipity philosophy, i.e. it does not target a specific object but is going to fly out to collect data about objects that are, for the most, unstudied and unobserved so far.

Several possible interplanetary orbits may be used for Bering. The simplest solution is to let Bering fly into an interplanetary orbit with aphelion at about 3.5 AU (mean semimajor axis of the main asteroid belt) and perihelion at about 0.7 AU (Venus semimajor axis). This orbit can be achieved with a single unpowered gravity assist maneuver from Venus whereas the V required to reach Venus could be delivered directly by the launcher.

Such an orbit has a period of approximately three years out of which almost two will be spent in the transfer from the Earth-Venus region to the main belt and back. Only less than three months will be spent in the Earth-Venus region. Observations in not expected areas, i.e. in the transfer part of the orbit are quite likely and very valuable but given the nature of the mission, a different approach that maximizes the permanence in the interesting region is to be preferred.

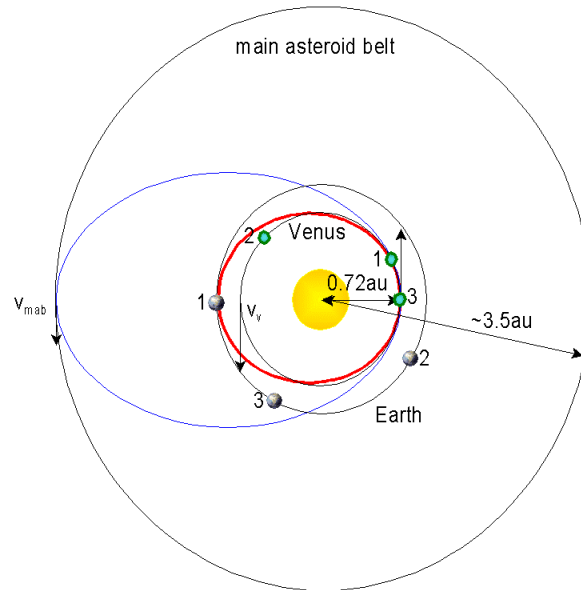


Figure 12: The mission profile. Planets and asteroids orbits are shown circular and coplanar for simplicity. The figure also show the positions of the Earth and Venus during the first phase of the mission and its assumes a fly-by at the second passage of the perihelion (1.5 period).

The proposed preliminary mission profile is sketched in Fig. 12 and can be broken down into three phases:

1. Study of the Earth-Venus region
2. Transfer to the main belt
3. Study of the main belt region

First phase: Earth-Venus and NEO's: During the first phase of the mission, Bering flies in an elliptical orbit between the Earth and Venus (red in Fig. 12). Taking advantage of the favorable illumination conditions, Bering will gather data and study the NEO's.

This orbit can be achieved directly by the launcher but shall rendezvous with Venus only at the second or third perigee passage in order to allow enough time to study the inner region. The period of this orbit is ~280 days.

Second phase: Venus-Main Asteroid Belt and “who knows”: The second phase starts with a Venus fly-by that injects Bering in its course toward the main asteroid belt (blue in Fig. 12). The transfer will last approximately one year. During this phase the instruments will be operating but it is difficult to estimate the possible scientific return.

Third phase: In the Main Asteroid Belt and selected targets: The goal of the third phase is to study the populations of asteroids in the main belt. The amount of observed objects depends on the actual spacecraft position and the distribution of the asteroids. Assuming, for the time being, that the observed bi-log distribution of asteroids (Fig. 5) extends to sub-kilometer objects, we expect to detect approximately one object/day. The number of detections outside this region needs to be reviewed in light of the expected distribution of the population.

The orbital position obviously affects the chance of observations because the asteroid distribution is not uniform. Nevertheless, as this is a discovery mission, observations in not expected areas are quite likely and very valuable.

In order to be able to move through the belt, one possible solution would be to have the perifocus at 2.2 AU and the apofocus at 3.5. The ΔV required to “circularize” the orbit at the main belt is approximately 6.5km/s. This and other solutions need to be carefully investigated and analyzed.

6. Platform requirements

We propose that Bering should be a slow spinning mission, this requires a symmetric body. As Bering will bring tanks for its cold gas propulsion system, these tanks need to be arranged symmetrically and depleted at the same rate throughout the mission in order to keep the spacecraft balanced. This leads to the spacecraft design sketched in Fig.13 below.

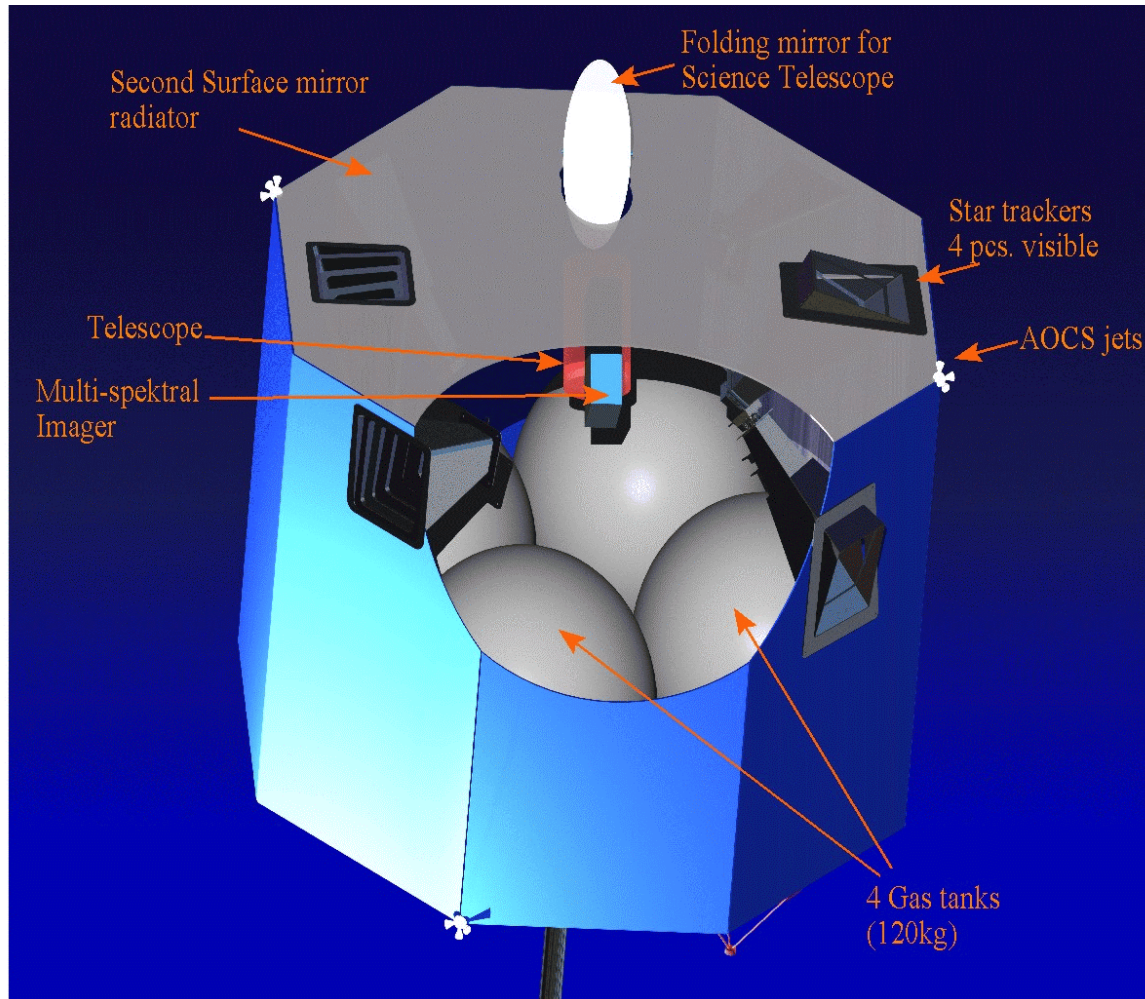


Figure 13: *Artistic impression of the Bering preliminary design.*

It is proposed to attach the parabolic Earth communications antenna on the top surface of the body with a fixed pointing in the direction of the spacecraft symmetry axis. This implies that the spin axis shall always be pointed towards the Earth. The slow spin of the spacecraft and the modest angular speed at which the rotation axis shall be realigned to track the Earth continuously, makes it an easy task for the attitude control system to accomplish this using its small thrusters.

No specific standard platform has been identified at this stage which can be adapted to the Bering mission. However, Bering bears significant resemblance with the Meteosat Second Generation (MSG) satellites, although

these are fast spinners with a cylindrical body. Throughout the design phase, design concepts, components and subsystems having a flight heritage will be preferred in order to minimize risk.

6.1. Power budget

The proposed orbit will take Bering out to 3.5 AU where the sunlight intensity is only 8.1% of that in Earth orbit. This implies that a large solar panel area is needed. For reasons of pointing stability it is not desirable to have deployable solar panels. Therefore, body-mounted panels are needed. The power budget is based on a rotationally symmetric body with an octagonal cross-section, cf. Fig. 13. All surfaces are covered with solar cells to the largest extent possible. The proposed width of the octagon is 2.0 m and the proposed height of the body is 1.75 m.

In order to maximize available power at aphelion, it is proposed to use triple-junction InGaP/GaAs/Ge solar cells having a 26% efficiency at BOL. Various factors, which shall be quantified with a higher confidence during the study, leads to a worst case available bus power at worst case attitude of 51.4 W.

The cruise phase is intended to cover power consumption during routine observations with continuous low speed Earth telemetry contact. During this phase only 1 W RF is output from the transmitter saving power to enable operation at aphelion.

Campaigns include intensive data taking using the multispectral imager and laser ranger e.g. during an asteroid rendezvous including ejection and tracking of a Magnetometer Free Flyer. High Speed Downlink mode includes downlinking of a large number of stored images. This phase can be supported for a limited time e.g. 1-2 hours near aphelion due to stored energy in a battery suitably sized to supply the approx 24 W/hour deficit in the aphelion power budget. The power margin at aphelion should enable charging of the battery at about half the rate at which it is depleted during high-speed downlink mode.

6.2. Telemetry downlink budget

Establishing a communications link at the maximum Earth-Bering separation of 4.5 AU with a power-constrained spacecraft is no simple issue.

Noting that a line-of-sight link using aperture antennas at both transmitting and receiving ends allows a quadrupling of bit rate every time carrier frequency is doubled, everything else equal, leads us to propose a Ka-band link with a nominal carrier frequency of 32 GHz.

The estimates are based on information on ESA's tracking station network and the NASA Deep Space Network (DSN).

It is found that even a 5 m ground station can support a modest bit rate with Bering even at aphelion and the Earth in opposition to the sun seen from Bering. In Low Power mode the max. sustainable bit rate figures are 1/10 of those in high power mode. This implies that a 5 m ground station is not a viable solution for this scenario. However, when Bering is within 2.8 AU from the sun, the power margin is positive for the high power telemetry downlink case. This is the case for around half the 1112 day orbit period. The high power mode can thus be sustained continuously for 50% of the orbit period and intermittently for the rest of the time.

In high power mode the net downlink capacity is around 800 kbytes/hour at aphelion and around 1.8Mbytes/hour at 3 AU using a 34 m ground station. This is inferred from calculations assuming approximately 10% formatting overhead.

7. Conclusion

A deep space mission to detect and characterize sub-kilometer objects between Jupiter and Venus has been proposed. The scientific rationale for such a mission has been presented and focus is on the investigation of asteroid evolution and determination of meteorite parenthood.

The technological means for such a deep space mission has been presented. They include advanced stellar compasses, multi spectral imager, laser ranger and magnetometer probes.

The Bering mission analysis is currently ongoing.

References

- Bell et al. (1989) Asteroids: The big picture. In Asteroids II (Binzel, Gehrels and Matthews, Eds.) 921-945, University of Arizona Press, Tucson.
- Binzel R. P. and Xu S. (1993) Chips off of asteroid 4 Vesta - Evidence for the parent body of basaltic achondrite meteorites. *Science* 260, 186-191.
- Bottke W.F., Morbidelli A., Jedicke R., Petit J-M., Michel P., and Metcalfe T.S. (2002) Debiased orbital and absolute magnitude distribution of the Near Earth Objects. Submitted to *Icarus*.
- Davis D.R., Farinella P., Marzari F., (1997), Lunar and Planetary Science Conference 28, 287
- Farinella P., Vokrouhlický D., and Hartmann W.K. (1998) Meteorite delivery via Yarkovsky orbital drift. *Icarus* 132, 378-387.
- Froeschle, C and Greenberg, R., (1989), In: Asteroids II, University of Arizona Press, 1989, p. 827-844
- Froeschlé C. and Morbidelli A. (1994) The secular resonances in the Solar system. IAU Symp. 160: Asteroids, Comets and Meteors 1993.
- Haack H., Farinella P., Scott E.R.D., and Keil, K. (1996) Meteoritic, asteroidal, and theoretical constraints on the 500 Ma disruption of the L Chondrite parent body. *Icarus* 119 182-191.
- JHU/APL Technical Digest, Vol 19, # 2 (1998) NEAR Laser Rangefinder
- Keil K., Haack H. and Scott E.R.D. (1994) Catastrophic fragmentation of asteroids: evidence from meteorites. *Planet. Space Sci.* 42 1109-1122.
- Kivelson M.G., Bargatze L.F., Khurana K.K., Southwood D.J., Walker R.J., Coleman P.J.Jr., (1993), *Science* 271, 331
- Moons M. (1997) Review of the dynamics in the Kirkwood gaps. *Celestial mechanics and Dynamical Astronomy* 65, 175-204.
- Morbidelli A. et al., (2000), Understanding the distribution of Near-Earth Objects, ESA Contract no. 14018/2000/F/TB
- Schmitz B., Peucker-Ehrenbrink B., Lindström M., and Tassinari M. (1997) Accretion rates of meteorites and cosmic dust in the early Ordovician. *Science* 278, 88-90.
- Sugiura N., Strangway D.W., (1988), in *Meteorites and the Early Solar System* (eds.) J.F. Kerridge, M.S. Matthews, University of Arizona Press, Tucson, 595.
- Sykes M.V. et al. (2000), The 2MASS asteroid and comet survey. *Icarus* 146, 161-175.